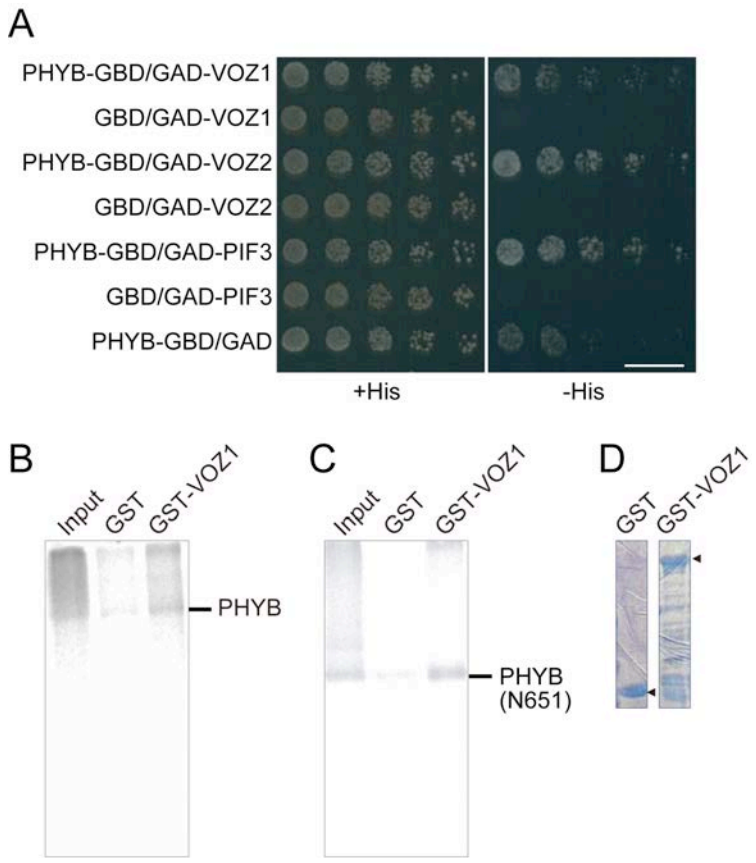

Supplemental Figure 1. Interaction of VOZ proteins with phyB.

(A) Specific interaction of VOZ proteins with phyB. Serial dilutions ($\times 3^{-2}$ to $\times 3^{-6}$) of transformed yeast cells were grown on nonselective +His (-Trp/-Leu) and selective -His (-His/-Trp/-Leu, containing 0.2 mM 3-amino-1,2,4-triazol) medium. GBD, Gal4 DNA-binding domain; GAD, Gal4 activation domain; PIF3, phytochrome-interacting factor 3. Bar = 1 cm. (B-D) *In vitro* binding of VOZ1 protein to PHYB (B) and to PHYB N-terminal domain [PHYB (N651)] (C). ^{35}S-labeled PHYB and PHYB (N651) synthesized by *in vitro* transcription/translation was incubated with either GST or GST-VOZ1 immobilized on glutathione sepharose beads, and proteins retained on the beads were resolved by SDS-PAGE. The interactions of full-length PHYB with VOZ1 (B), and N-terminal domain of PHYB, which is crucial for signaling (Matsushita et al., 2003), with VOZ1 were confirmed (C). One third the amount of GST and GST-VOZ1 proteins used in these experiments was loaded and stained. (D). The arrows indicate the purified protein.

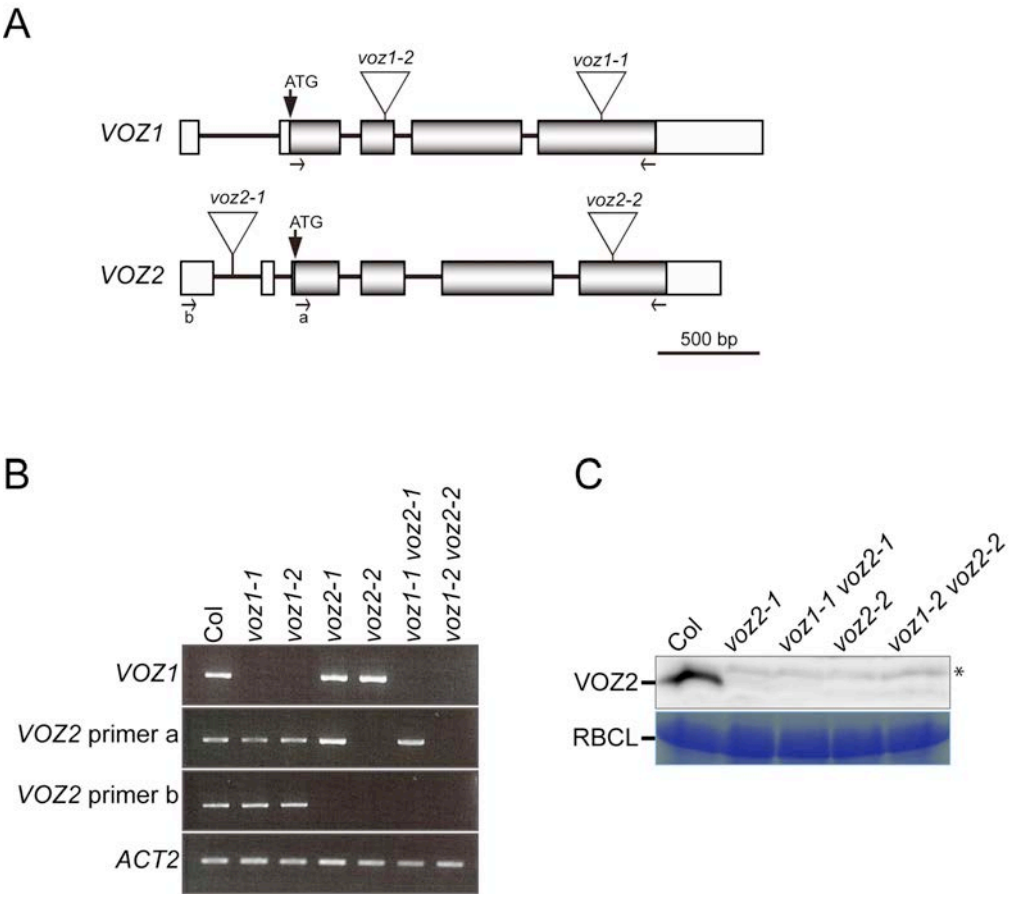

Supplemental Figure 2. T-DNA insertional mutants for *VOZ* genes.

(A) Schematic illustration of the exon–intron structure of *VOZ* genes. Exons are represented by boxes, translated regions are shaded, introns are lines, and T-DNA insertions are triangles. The primers used to detect the transcripts are indicated by arrows. (B) *VOZ1* and *VOZ2* mRNA expression was detected by RT-PCR. *ACT2* was amplified as an internal control. Thirty PCR cycles were run. (C) VOZ2 protein expression in Col, *voz2-1*, *voz1-1 voz2-1*, *voz2-2* and *voz1-2 voz2-2* mutants. Plants were grown under continuous white light for 10 d. Proteins were subjected to gel blot analysis with anti-VOZ2 antibody. CBB staining of Rubisco large subunit (RBCL) is shown as a loading control. Asterisk represents non-specific detection.

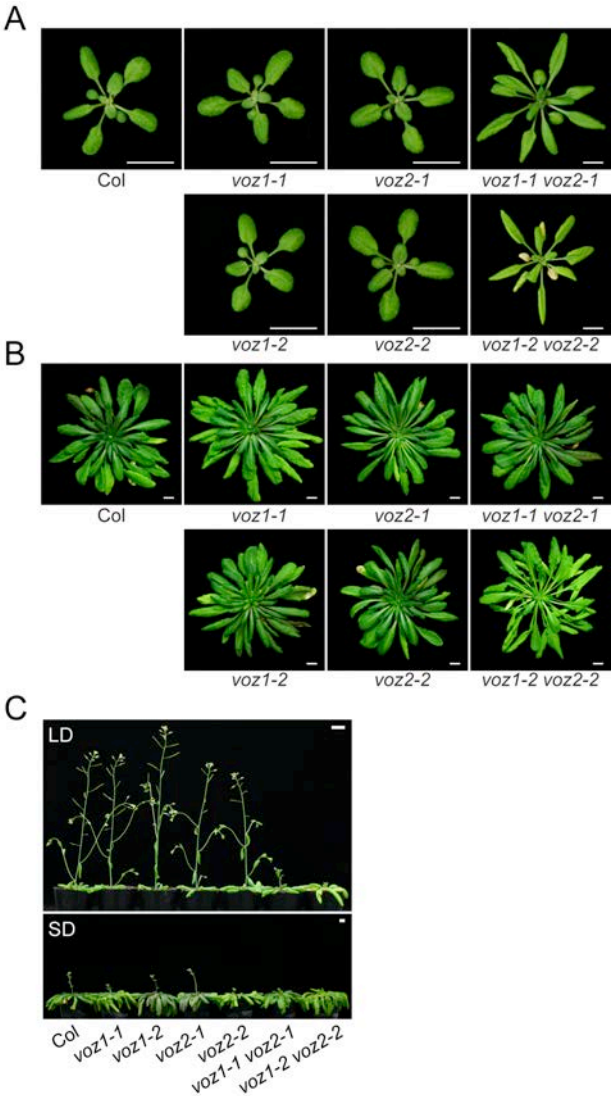

Supplemental Figure 3. Phenotype of *voz* mutants grown under LD or SD conditions.

(A and B) Plants at bolting. (A) Plants were grown under LD conditions for 16 d (Col, *voz1-1*, *voz1-2*, *voz2-1* and *voz2-2*) or 24 d (*voz1-1 voz2-1* and *voz1-2 voz2-2*). (B) Plants were grown under SD conditions for 70 d. (C) Flowering phenotype under LD or SD conditions. Plants were grown under LD conditions for 30 d (top). Plants were grown under SD conditions for 75 d (bottom). Bars = 1 cm.

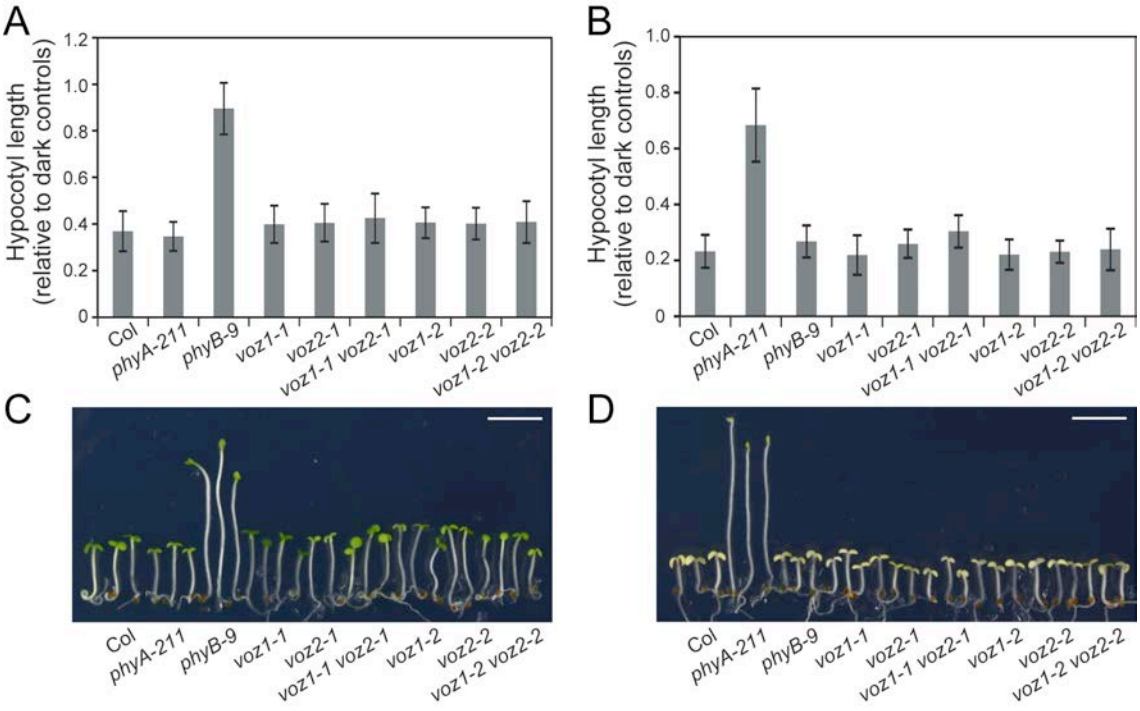

Supplemental Figure 4. Hypocotyl length phenotype of *voz* mutants.

Hypocotyl length of *voz1*, *voz2*, and *voz1 voz2* double mutants grown under red (A and C) or far-red (B and D) light for 5 d. (A, B) Hypocotyl elongation is presented as a percentage of elongation relative to dark-grown seedlings of the same genotype. Data are the mean ± s.d. ($n \geq 10$). (C, D) Images of seedlings. Bars = 5 mm.

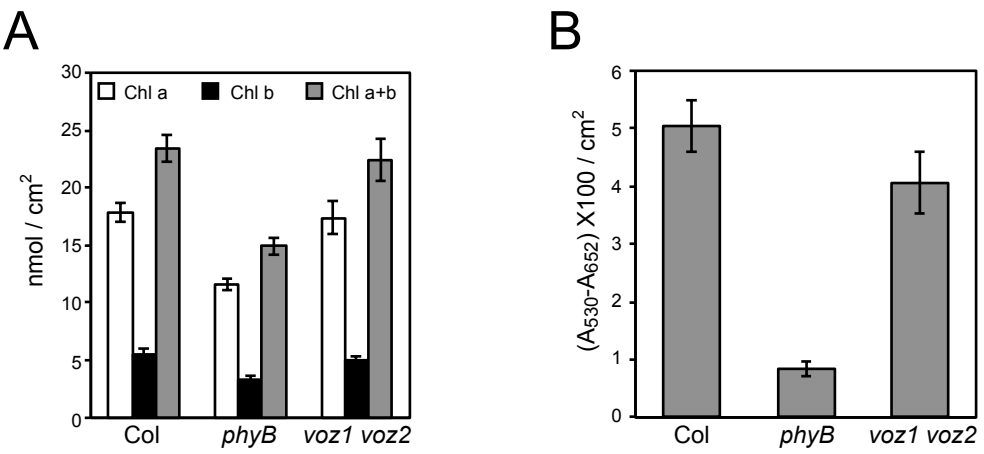

Supplemental Figure 5. Chlorophyll and anthocyanin accumulation levels.
(A) Determination of chlorophyll contents. 0.126 cm^2 leaf materials from 17-d-old plants were ground in liquid nitrogen and extracted in methanol. Chlorophyll contents were determined by measuring the absorbance at 652 nm and 665 nm. The equations derived from Porra et al. (1989) were used to estimate the concentrations of chlorophyll a (Chl a), chlorophyll b (Chl b), and total chlorophyll (Chl a+b). Data are the mean ± s.e. (*n* = 5). (B) For anthocyanin measurement, 0.126 cm^2 leaf materials from 20-d-old plants were ground in liquid nitrogen and extracted in methanol including 1% of HCl, purified by 70% chloroform treatment. Two absorbances (A_{530} and A_{652}) of the extracts were measured spectrophotometrically, and the amount of anthocyanin was calculated as (A_{530}–A_{652}) X 100 / cm^2 leaf. Data are the mean ± s.e. (*n* = 10).

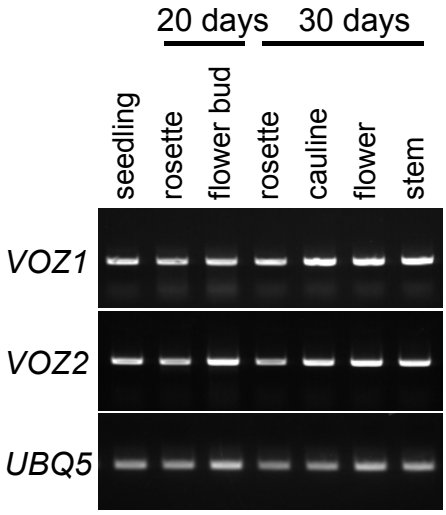

Supplemental Figure 6. *VOZ* gene expression patterns.

RT-PCR analysis of *VOZ* gene expression in various organs of Col plants grown under LD for 20 or 30 d. *UBQ5* was used as a loading control. *VOZ1* and *VOZ2* were ubiquitously expressed in all organs examined.

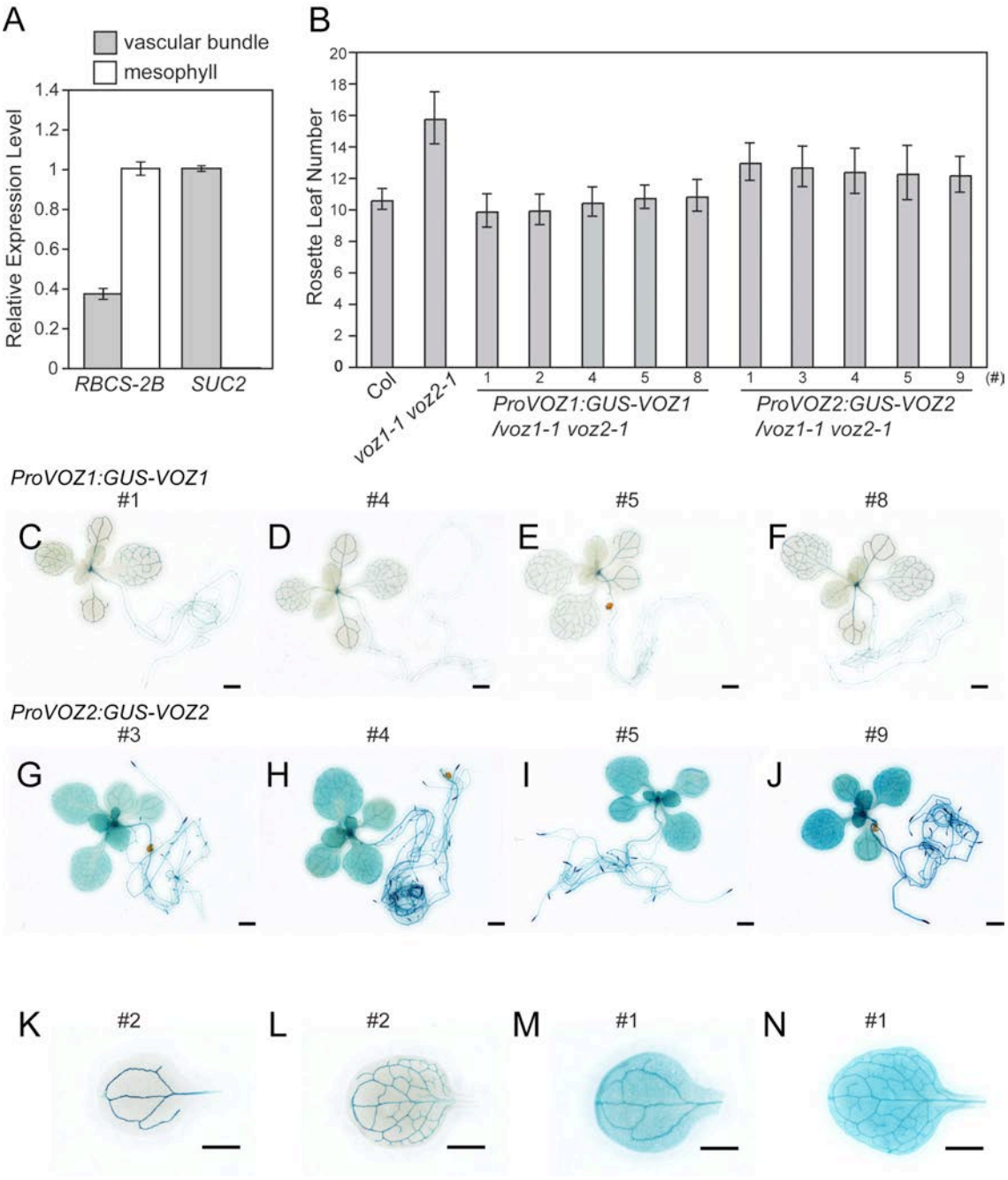
A
vascular bundle
mesophyll
Relative Expression Level
RBCS-2B
SUC2
B
Rosette Leaf Number
Col
voz1-1 voz2-1
ProVOZ1:GUS-VOZ1 /voz1-1 voz2-1
ProVOZ2:GUS-VOZ2 /voz1-1 voz2-1
(#)
ProVOZ1:GUS-VOZ1
C #1
D #4
E #5
F #8
ProVOZ2:GUS-VOZ2
G #3
H #4
I #5
J #9
K #2
L #2
M #1
N #1

Supplemental Figure 7. Complementation test and GUS staining of *ProVOZ:GUS-VOZ/voz1 voz2* transgenic plants.

(A) Expression of *RBCS* (a mesophyll maker) and *SUC2* (a vascular bundle maker) in the mesophyll and vascular bundle samples. Seedlings were grown under LD conditions for 10 d. *ACT2* was used as a control. RNA extraction was performed three times independently. Data are the mean ± s.e. (n = 3). (B) Rosette leaf number at bolting of *ProVOZ1:GUS-VOZ1/voz1 voz2* and *ProVOZ2:GUS-VOZ2/voz1 voz2* lines. Plants were grown under LD conditions. Data are the mean ± s.d. ($n \geq 15$). (C–N) GUS expression patterns of *ProVOZ1:GUS-VOZ1* (C–F, K, L) and *ProVOZ2:GUS-VOZ2* (G–J, M, N) transgenic LD-grown seedlings on day 10 in whole seedlings (C–J), cotyledons (K, M) and the first true leaves (L, N). Bars = 1 mm.

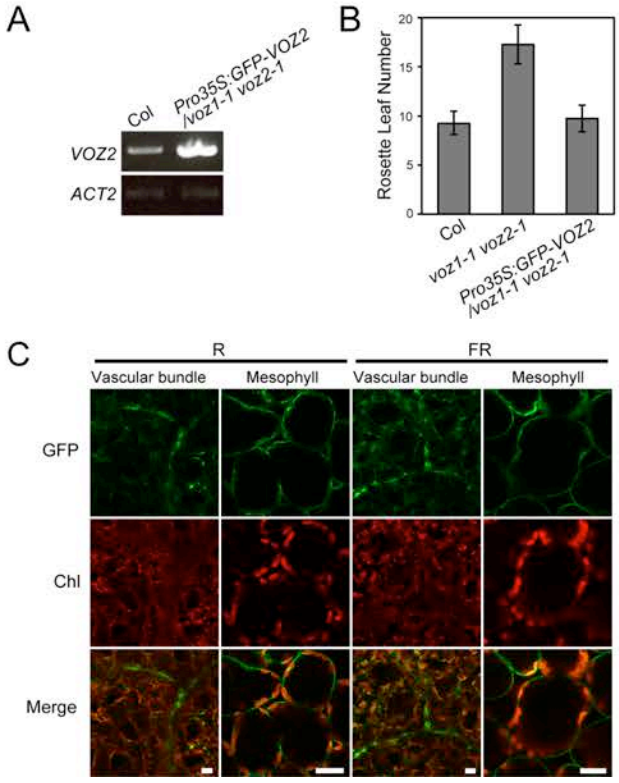

Supplemental Figure 8. Subcellular localization of GFP-VOZ2 fusion protein under different light conditions.

(A) mRNA levels of *VOZ2* in the *Pro35S:GFP-VOZ2-NLS/voz1 voz2* line was compared with that of Col. Plants were grown under continuous white light for 10 d. The samples were analyzed by RT-PCR. *ACT2* was amplified as an internal control. The PCR amplification comprised 25 cycles. (B) Rosette leaf number at bolting of the *Pro35S:GFP-VOZ2/voz1 voz2* line grown under LD conditions. Data are the mean ± s.d. ($n \geq 14$). (C) Confocal microscopic images of GFP, chloroplast autofluorescence (Chl) and GFP-Chl merged images (Merge) from vascular bundle cells and mesophyll cells in leaves of *Pro35S:GFP-VOZ2/voz1 voz2* plants. Seedlings were grown under continuous white light for 10 d and treated with either red (R) or far-red (FR) light for 24 h. Bars = 20 μm.

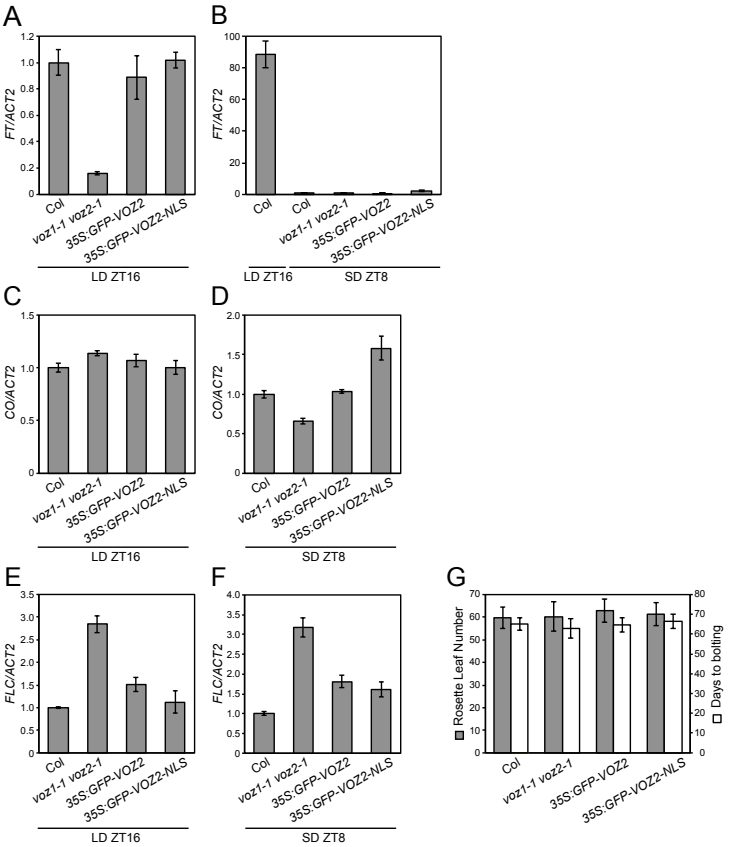

Supplemental Figure 9. Relative expression levels of *FT*, *CO* and *FLC*, and flowering time in *VOZ2* overexpression lines.

Relative expression levels of *FT* (A, B), *CO* (C, D) and *FLC* (E, F) determined by qRT-PCR in Col, *voz1 voz2* mutant, *Pro35S:GFP-VOZ2/voz1 voz2* and *Pro35S:GFP-VOZ2-NLS/voz1 voz2 #7*. Plants were grown for 10 d under LD conditions (A, C, E) or grown under SD conditions for 20 d (B, D, F). RNA was extracted from rosette leaves at ZT16 (A, C, E) or at ZT8 (B, D, F). *ACT2* was used as a control. RNA extraction was performed three times independently. Data are the mean ± s.e. (*n* = 3). (G) Rosette leaf number and number of days to bolting of Col, *voz1 voz2* mutant, *Pro35S:GFP-VOZ2/voz1 voz2* and *Pro35S:GFP-VOZ2-NLS/voz1 voz2 #7* grown under SD conditions. Data are the mean ± s.d. (*n* ≥ 12).

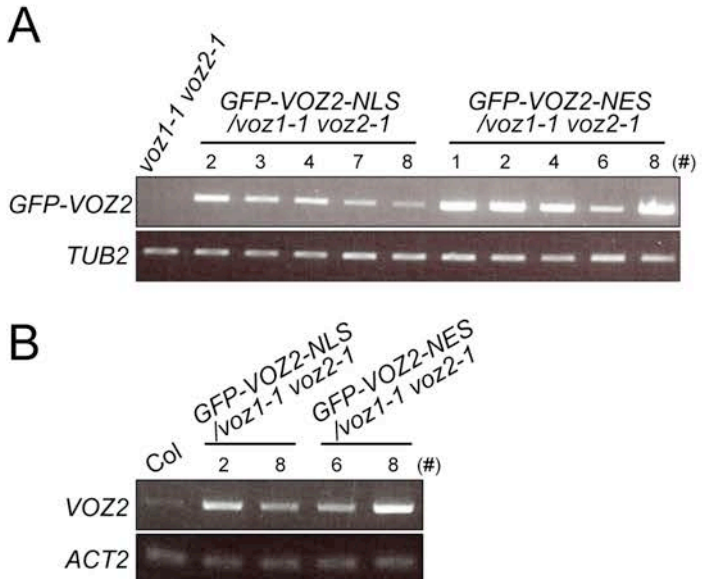

Supplemental Figure 10. Expression of *GFP-VOZ2* mRNA in NLS and NES lines.

(A) mRNA levels of *GFP-VOZ2* in the *Pro35S:GFP-VOZ2-NLS/voz1 voz2* and *Pro35S:GFP-VOZ2-NES/voz1 voz2* lines. Plants were grown under LD conditions for 10 d. The samples were analyzed by RT-PCR. *TUB2* was amplified as an internal control. The PCR amplification comprised 25 cycles.

(B) mRNA levels of *VOZ2* in the *Pro35S:GFP-VOZ2-NLS/voz1 voz2* and *Pro35S:GFP-VOZ2-NES/voz1 voz2* lines were compared with that of Col. Plants were grown under LD conditions for 10 d. The samples were analyzed by RT-PCR. *ACT2* was amplified as an internal control. The PCR amplification comprised 25 cycles.

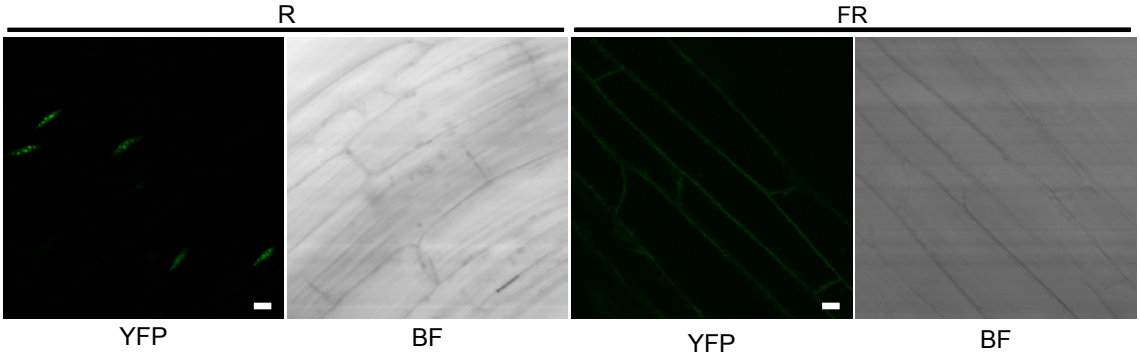

Supplemental Figure 11. Subcellular localization of phyB-YFP in Arabidopsis.

Confocal images of YFP and bright-field (BF) images from *Pro35S:phyB-YFP/phyB* transgenic line. Plants were grown under dark conditions for 3 d and exposed to red (R) or far-red (FR) light for 2 d. Fluorescence from YFP (observation, 520 to 560 nm; excitation, 515 nm) was observed after the light treatment. Fluorescent signals and bright-field images were captured using a confocal laser scanning microscope (FluoView 1000, Olympus). Bars = 10 μm.

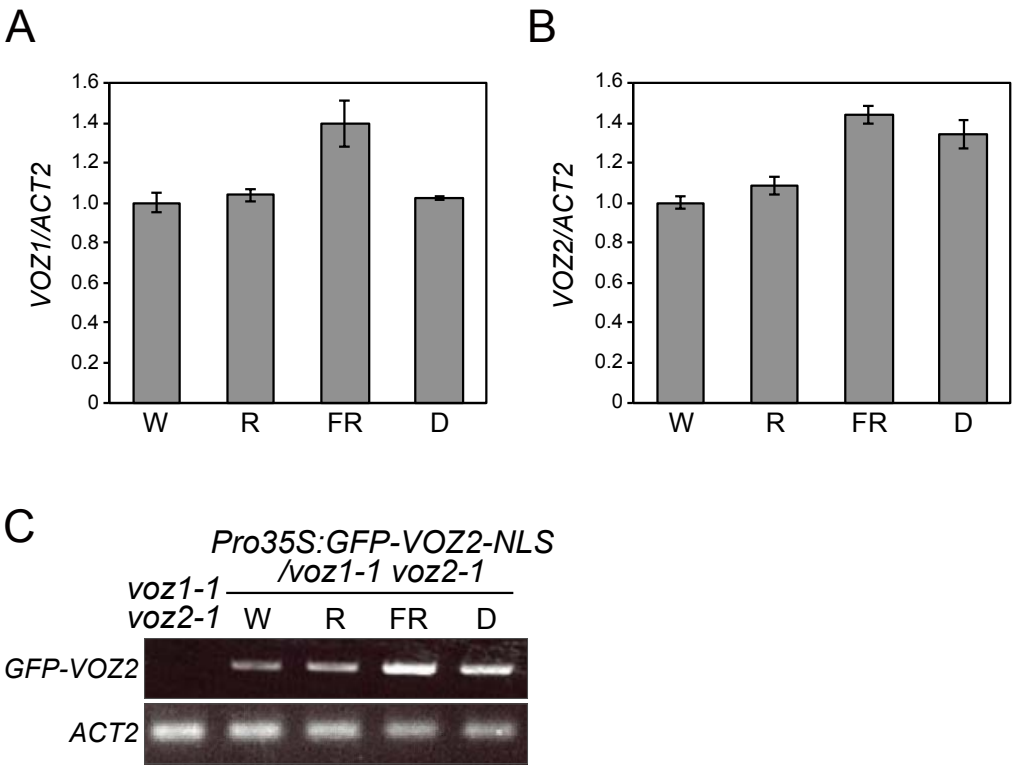

Supplemental Figure 12. Expression of *VOZ* mRNA under different light conditions.

(A, B) mRNA levels of *VOZ1* (A) and *VOZ2* (B) in Col were measured by qRT-PCR. Plants were grown under continuous white light for 10 d and treated with either white (W), red (R), or far-red (FR) light, or darkness (D) for 24 h. *ACT2* was used as a control. RNA extraction was performed three times independently. Data are the mean ± s.e. (*n* = 3). (C) mRNA levels of *GFP-VOZ2* in the *Pro35S:GFP-VOZ2-NLS/voz1 voz2* line. Plants were grown under continuous white light for 10 d and treated with either W, R, FR, or D for 24 h. The samples were analyzed by RT-PCR. *ACT2* was amplified as an internal control. The PCR cycles was 23.

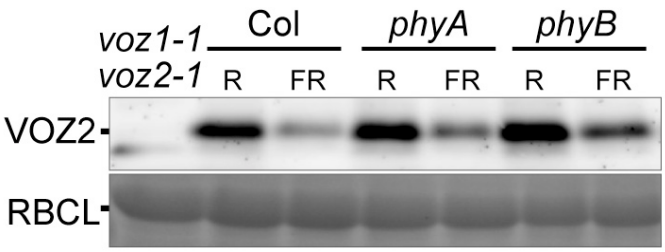

Supplemental Figure 13. VOZ2 protein accumulation levels in *phy* mutants under different light conditions.

VOZ2 protein levels in Col, *phyA* and *phyB*. Plants were grown under continuous white light for 10 d and treated with either red or far-red light for 24 h. Each lane contained 65 µg of total protein.

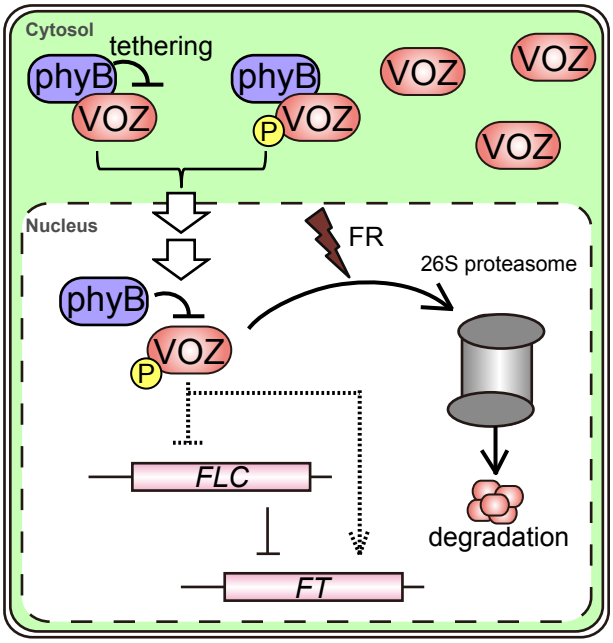

Supplemental Figure 14. Schematic illustration of a model for VOZ function.

Our data suggest that the function of VOZ protein is regulated by its limited translocalization and subsequent turnover in the nucleus. In the cytoplasm, VOZ proteins interact with phyB (Figure 6), which may tether VOZ proteins within the cytoplasm or be involved in modification of the VOZ protein, such as phosphorylation (Figure 7E). In the nucleus, VOZ protein turnover is promoted under far-red light conditions (Figure 7B). Genetic data show that *VOZ* promotes flowering downstream of phyB (Figure 1), regulating the expressions of flowering related genes, such as *FT* and *FLC* (Figure 3). P; Phosphorylation.

Supplemental Table 1. PCR primers used in the expression analysis

Genes	Forward sequence	Reverse sequence	Usage	Figure
RBCS	ACAAACAAGTAAGTAAGAGAAAAACC	AAGAAGCGGATGACTTCAAG	Real time	Fig. S7
SUC2	AAAACCCTCTCAAAGAAATTTC	ATATGATCTTACGAAGCCGTTC	Real time	Fig. S7
VOZ1	CACTAACACCACCAACAACAACAA	TCCATAGTCATTTGCCTGCTCTAC	Real time	Figs. 2 and S12
VOZ2	TCCTGCGGCTTTGAGGA	GGAGCGGAGTTTATGCTTGG	Real time	Figs. 2 and S12
FT	TATGATACGAGTAACGAACGG	AACACTCTCATTTTCCTCCC	Real time	Figs. 3 and S9
CO	GCTCCCACACCATCAAACTT	GTCGTGCCCTGTTGTTCTCT	Real time	Figs. 3 and S9
FLC	CCGAACTCATGTTGAAGCTTGTTGAG	CGGAGATTTGTCCAGCAGGTG	Real time	Figs. 3 and S9
ACT2	TCAGATGCCCAGAAGTCTTGTTCC	CCGTACAGATCCTTCCTGATAT	Real time, RT-PCR	Figs. 2, 3, S2, S7, S8, S9, S10, and S12
GFP-VOZ2	TGGTCCTGCTGGAGTTCGT	GTCCCAGAAAAGCAGATGGAGG	RT-PCR	Figs. S10 and S12
TUB2	CTCAAGAGGTTCTCAGCAGTA	TCACCTTCTTCATCCGCAGTT	RT-PCR	Fig. S10
VOZ1	ATGACGGGGAAGCGATC	TCAGGGGATATAATAGTCGCTTAG	RT-PCR	Fig. S2
VOZ2a	ATGTCAAACCACCCGAAGAT	TCACTCCTTACGACCTTTGGT	RT-PCR	Fig. S2
VOZ2b	ATCGTCGCTCTCTGTTTGC	TCACTCCTTACGACCTTTGGT	RT-PCR	Fig. S2
VOZ1	TTTGGTTCAGGGGAAGTCAG	ACGCGTCGACTCAGGGGATATAATAGTCGC	RT-PCR	Fig. S6
VOZ2	AGCATAAACTCCGCTCCTGA	CCGCTCGAGTCACTCCTTACGACCTTTG	RT-PCR	Fig. S6
UBQ5	GTGGTGCTAAGAAGAGGAAGAA	GCTACAACAGATCAAGCTTC	RT-PCR	Fig. S6
VOZ2	ATGTCAAACCACCCGAAGAT	GTCCCAGAAAAGCAGATGGAGG	RT-PCR	Fig. S8, S10

Supplemental References

Matsushita, T., Mochizuki, N., and Nagatani, A. (2003). Dimers of the N-terminal domain of phytochrome B are functional in the nucleus. Nature **424,** 571-574.

Porra, R., Thompson, W., and Kriedemann, P. (1989). Determination of accurate extinction coefficients and simultaneous equations for assaying chlorophylls a and b extracted with four different solvents: verification of the concentration of chlorophyll standards by atomic absorption spectroscopy. Biochim. Biophys. Acta **975,** 384-394.